

Sigma-like phase and nanoscale segregation in polycrystalline $\text{Fe}_x\text{Cr}_{1-x}$ films: An element-resolved magnetic and structural study

J. B. Kortright, Sang-Koog Kim, and H. Ohldag*

Materials Sciences Division, Lawrence Berkeley National Laboratory, University of California, Berkeley, California 94720

(Received 12 August 1999)

Complex changes in room-temperature magnetic and chemical order in sputtered $\text{Fe}_x\text{Cr}_{1-x}$ films ($1.0 > x > 0.24$) are revealed by resonant soft x-ray magneto-optical and scattering spectroscopies. A distorted, homogeneous paramagnetic phase at $x \cong 0.55$, similar to the bulk σ phase, is found. Linked chemical and magnetic segregation on either side of this phase are interpreted in terms of favorable and frustrated exchange interactions, as is a net Cr local moment for $x \geq 0.69$. Segregated alloys exhibit reversible magnetization originating from weakly coupled, noncollinear Fe spins.

$\text{Fe}_x\text{Cr}_{1-x}$ alloys are interesting among binary magnetic alloys because the different d -band filling of the isostructural elements yields room-temperature ferromagnetic (FM) order in Fe and spin-density wave (SDW) antiferromagnetic (AFM) order in Cr. The transition from FM to SDWAFM order with x is not well understood, especially in thin films where few techniques can resolve elemental contributions to magnetic and chemical ordering in films tens of nanometers thick. Alloy films are relevant to Fe/Cr multilayers exhibiting giant magnetoresistance,¹⁻³ and to the coupling of Fe and Cr across interfaces and in layered structures,⁴⁻¹⁰ since alloying of Cr on Fe(001) appears related to Cr ordering and inter-layer coupling.^{7,8} Fe on Cr(001) orders in orthogonal directions depending on the substrate surface step density¹¹ indicating high sensitivity to structural disorder. Possible similarities to Co-Cr based films used in magnetic recording further motivate study of Fe-Cr films. Here element-resolved soft x-ray magneto-optical and scattering techniques provide unique information that reveal complex changes in magnetic order with composition that correlate with changes in chemical and structural order.

Bulk $\text{Fe}_x\text{Cr}_{1-x}$ alloys exhibit rich metastable behavior depending on x and preparation,¹² while thin films have received less study. Fe and Cr have less than 1% difference in room-temperature (T_R) bcc lattice constant, yet a continuous series of solid solutions exists only above 1093 K. The σ phase is stable for $0.57 < x < 0.51$ and $1093 \text{ K} > T \geq 713 \text{ K}$, while at lower T samples in this range can exhibit a miscibility gap between chemically segregated bcc phases. Bulk magnetic ordering temperatures above T_R include FM T_C for $x > 0.3$ and SDWAFM T_N for $x < 0.02$ for bcc alloys, while the σ phase is paramagnetic (PM) at T_R . Neutron scattering revealed an inversion in chemical short-range order whereby Cr prefers Fe nearest neighbors for $x > 0.9$ and clusters for smaller x .¹³ In thin films no reports of the σ phase are evident. A miscibility gap between bcc phases was interpreted from a split diffraction peak in annealed films,¹⁴ and from annealing-enhanced magnetoresistance.¹⁵ A reversible susceptibility in films was interpreted to result from slight out-of-plane anisotropy.¹⁶ This study reveals a σ -like phase at T_R , linked chemical and magnetic segregation interpreted in terms of stable and frustrated exchange interactions, and evidence for noncollinear Fe moments in segregated samples.

Polycrystalline films were grown by rf magnetron sputtering onto oxidized Si wafer and SiN_x membrane substrates at ambient T . Varying the surface area ratio of Fe and Cr target material varied X , and an amorphous SiC capping layer prevented oxidation. Areal mass density of Fe and Cr was determined by x-ray fluorescence, yielding $x = 1.0, 0.91, 0.85, 0.69, 0.58, 0.50, 0.39, 0.34$, and 0.24 . Thickness t varied from 55 to 75 nm, as determined by fitting oscillations in low-angle x-ray reflectivity, and is 10 or more times thinner than films studied in Refs. 14-16. All data are collected at T_R .

Transmission soft x-ray magneto-optical (MO) techniques near the Fe and Cr $2p_{3/2}(L_3)$ and $2p_{1/2}(L_2)$ levels yield magnetic signals roughly proportional to the net moment or magnetization of each element along the wave vector \mathbf{k} . The complex Faraday MO response is $(n_+ - n_-)\pi t/\lambda$ where $n_{+/-} = 1 - \delta_{+/-} - i\beta_{+/-}$ are the refractive indices for opposite helicity (+/-) circular polarization, $\delta(\lambda)$ and $\beta(\lambda)$ are weighted sums of the real and imaginary parts of Fe and Cr atomic scattering factors,¹⁷ and λ is the wavelength. Magnetic circular dichroism (MCD) is $(\beta_+ - \beta_-)$. Spectra proportional to this quantity were obtained at $\theta = 45^\circ$ utilizing fixed helicity elliptical polarization from bending magnet beamlines by reversing magnetization \mathbf{M} with 180° rotation of samples and permanent magnets providing 700 Oe in-plane field \mathbf{H} . Absorption spectra $\mu t \cong -\ln(I/I_0)$ were normalized to have edge jump of 1 after pre-edge subtraction to yield a common, per atom scale. Their difference with reversed \mathbf{M} yields the spectra in Fig. 1. Minor thickness effects are present in some Fe MCD spectra, precluding their precise quantitative comparison.¹⁸ The spectra do show correct qualitative trends with x .

MCD spectra reveal that magnetization of Fe and Cr evolve differently with x . Cr exhibits a net moment that rapidly decreases with added Cr for $x \geq 0.69$. Fe retains a strong net moment for $x \geq 0.69$, a weak or zero moment for $x = 0.58$ and 0.50 , and a reduced moment for $x = 0.39$ and 0.34 decreasing to zero at $x = 0.24$. A zero MCD signal implies either AFM or PM order, and decreased net moments imply either uniform reduction for all atoms of a species, or an inhomogeneous distribution of moments. When present the Cr net moment opposes that of Fe, as indicated by the opposite sign of their spectra at E_F (the leading edge of the L_3 and L_2 lines) and consistent with studies of Cr moments

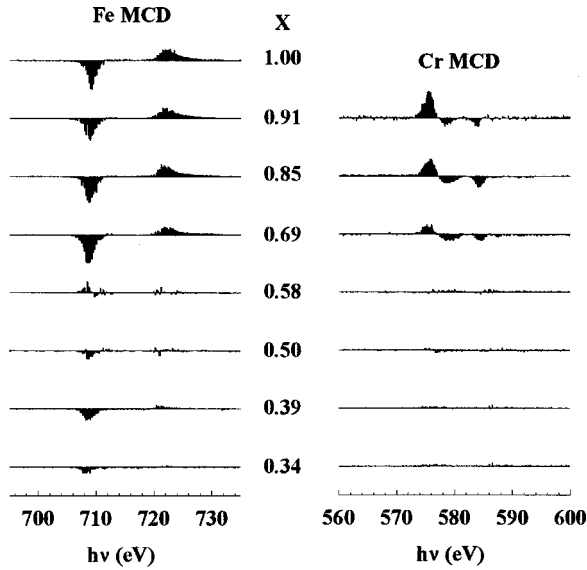


FIG. 1. Fe and Cr transmission MCD spectra taken in near-saturation field are normalized to common scale for each species. The L_3 and L_2 edges are at 708 and 720 eV for Fe, and at 574 and 584 eV for Cr.

in alloys^{12,13} and at surfaces.^{5,6} The unipolar and bipolar L_3 shapes of Fe and Cr, respectively, indicate that they retain distinctly different spin polarization in alloys, which is significant because d -state occupancy bears directly on the chemical potentials of Fe and Cr, which are thus spin-dependent properties.

Faraday rotation of linearly polarized radiation, given by $\alpha = (\delta_+ - \delta_-) \pi t / \lambda \sin \theta$, measures motion and approximate size of elemental magnetization. Element-specific hysteresis loops were obtained 2.5 eV below the L_3 lines in transmission ($\theta = 45^\circ$) while varying \mathbf{H} parallel to \mathbf{k} with an electromagnet. A tunable linear polarizer in the transmitted beam measures rotation α to exceed 10° near the Fe edge of Fe-rich samples.^{17,19} Elemental specific rotation, $\alpha_{\text{Fe,Cr}}^S = \alpha \sin \theta / tC$, provides a common measure of Fe ($C=x$) and Cr ($C=1-x$) magnetization for comparison between samples. Since Faraday rotation and MCD spectra are related by Kramers-Kronig transformation,¹⁷ the accuracy of comparison of elemental magnetization between samples using fixed-energy $\alpha_{\text{Fe,Cr}}^S$ is limited by the extent to which shapes of MCD spectra vary with x . Only if all spectra of Fe, e.g., differ only by energy-independent multiplicative factors do fixed-energy α_{Fe}^S loops rigorously measure relative Fe magnetization between samples. Distinct differences in MCD spectral shapes would indicate changing total or relative orbital/spin moments with X . Since elemental spectra in Fig. 1 have very similar shape, semiquantitative trends in elemental magnetization are obtained from Faraday loops.

Hysteresis loops normalized to $\alpha_{\text{Fe,Cr}}^S$ in Fig. 2 confirm MCD trends and reveal field-dependent similarities and differences in Fe and Cr magnetization. The identical coercive field H_C for Fe and Cr confirms that Cr species yielding the net moment are exchange-coupled to Fe. H_C increases from 8 Oe for pure Fe to a maximum of 35 Oe at $x=0.69$, indicating added resistance to reversal on alloying, but soft, low-anisotropy behavior in general. Both Fe and Cr have near zero susceptibility at $x=0.58$, indicating PM order, and

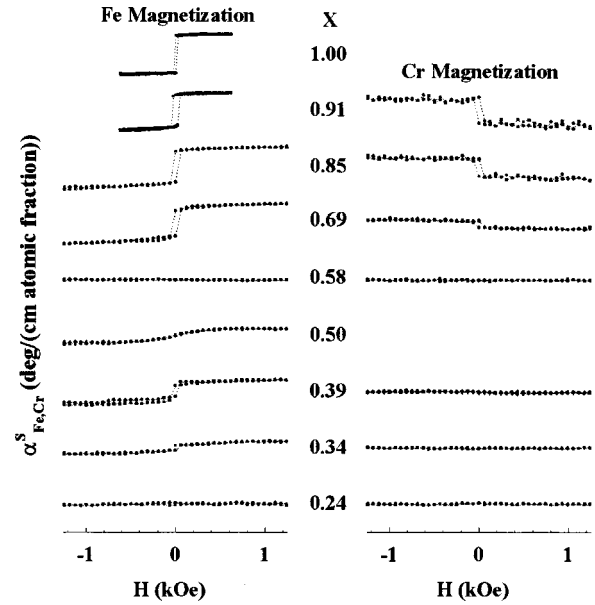


FIG. 2. Fe and Cr Faraday hysteresis loops normalized to an elemental specific rotation scale that provides a semiquantitative measure of elemental moment between samples. Data were collected at 2.5 eV below the L_3 edge of each element.

Cr susceptibility remains near zero for more Cr-rich alloys. Pure Fe exhibits weak reversible magnetization above H_C that is considerably increased in the alloys (except for $x=0.58$). The squareness $S = m_R / m_S$ provides a measure of this reversible magnetization. Here m_R and m_S are remnant and saturated elemental magnetization approximated by $\alpha_{\text{Fe,Cr}}^S$ measured at $\mathbf{H}=0$ and 650 Oe (a lower limit to the true saturated value), respectively, and normalized by α^S values at $x=1.0$ for Fe and $x=0.91$ for Cr loops. These relative elemental magnetization values in Fig. 3(a) summarize trends in Fe and Cr magnetization with x . Also plotted in Fig. 3(a) is $1-S$, that deviates appreciably from 0 only for Fe in a systematic way with X . An unusual magnetic state at $X=0.50$ is characterized by $1-S=0.9$, indicating predominantly reversible magnetization resulting from noncollinear moments.

Trends of Fe and Cr magnetization show that changes in magnetic order correlate with specific composition ranges. The discontinuity in Fe net moment at $x=0.58$ and the asymmetry in Cr net moment about this composition are not consistent with a continuous solution model, suggesting composition-dependent chemical segregation or changes in structure. Hard x-ray diffraction and soft x-ray resonant scattering reveal structural features that correlate with the changing magnetic order.

X-ray diffraction normal to the films reveals a pronounced lattice distortion at $x=0.58$ and 0.50 above a much smaller deviation above Vegard's law [Fig. 3(b)]. This noncubic distortion coincides with the σ phase stability range, where both the film and the bulk σ phase are paramagnetic at T_R . However, the films distorted lattice is not the same as that of the bulk σ phase. Even so, the simultaneous structural distortion and loss of magnetic order presumably have related microscopic origins.

Chemical ordering leading to clustering and segregation results in diffuse scattering peaked at or near the origin of

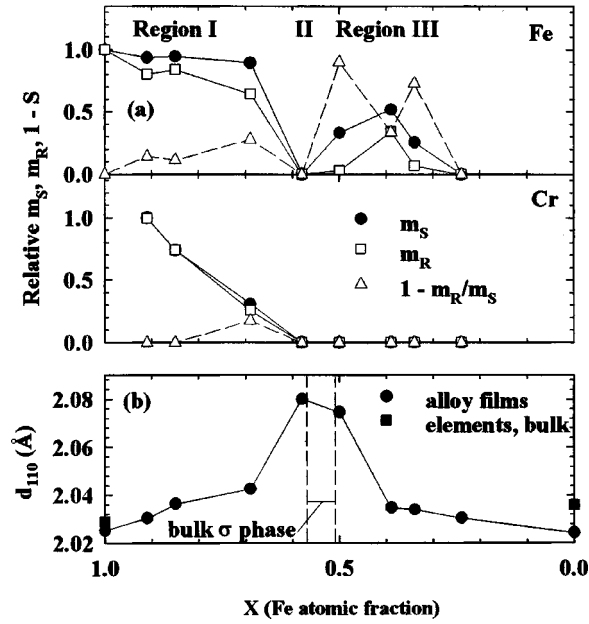


FIG. 3. (a) Relative saturated (m_S) and remnant (m_R) elemental magnetization obtained from Faraday elemental specific rotation $\alpha_{Fe, Cr}^S$. Also shown in $1-S$ where squareness $S = m_R/m_S$. Fe(Cr) results are in the top (bottom) panel. Lines connect data points. (b) Values for (110) interplanar spacing normal to the films. Solid lines connect measured data points. Regions I, II, and III correspond to distinct structural regions in the room-temperature phase diagram.

reciprocal space,²⁰ and was investigated by measuring resonantly enhanced scattering in transmission with scattering vector ($|\mathbf{q}| = 4\pi \sin \theta/\lambda$) in-plane from most samples and an uncoated SiN_x membrane. Figure 4 shows data measured 1 eV below the Fe L_3 peak and corrected for θ -dependent volume and absorption. The $x = 0.91, 0.85,$ and 0.69 alloys scatter well in excess of the substrate, while the $x = 0.58$ film scatters little more than the substrate. Energy scans at $q \cong 0.01 \text{ \AA}^{-1}$ show resonant enhancements of 10–100 times near the Fe $2p_{3/2}$ and $2p_{1/2}$ levels for $x \geq 0.69$, while Cr resonant enhancement systematically increases from zero at $x = 0.91$ with added Cr in this range. These resonant enhancements confirm that clustering or segregation contributes to the scattering for $x = 0.85$ and 0.69 . The film at $x = 0.58$ is relatively homogeneous, with no resonant enhancement at either edge. Resonantly enhanced scattering from segregation is strong at the Fe edge at $x = 0.50$ and decreases systematically with added Cr. Scattering was measured with samples at remnance following saturation, and contributions from both magnetic and chemical heterogeneity cannot be ruled out. Indeed chemical heterogeneity would presumably yield magnetic heterogeneity and hence magnetic contributions to scattering even with all moments saturated. The monotonic decrease of scattering for $x \geq 0.69$ is consistent with relatively uncorrelated scattering sources, while the peak for $x = 0.50$ away from $q = 0$ indicates interference between scattering centers spaced on average 50 nm apart in an interfering spherical particle model.

A consistent model of changing magnetic and chemical order with x , comprised of three distinct regions, emerges from the combined data. At $x = 0.58$ is a chemically homogeneous, paramagnetic phase with a distorted lattice. This is

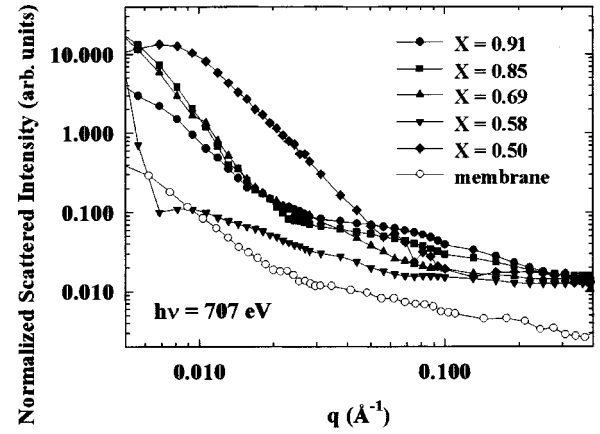


FIG. 4. Resonantly enhanced in-plane scattering measured 1 eV below the Fe L_3 edge from several alloy samples and a SiN_x membrane substrate.

a report of a phase analogous to the bulk σ phase in Fe-Cr films, and is henceforth termed the σ' phase. The σ' stability range of roughly $0.58 \geq x > 0.50$ comprises composition region II. Region I, comprising $1.0 > x > 0.58$, is the only region where Cr shows a net moment. At low concentrations in this range Cr appears to dissolve in Fe, while at higher concentrations it segregates. Region III comprises the Cr-rich samples $0.5 \geq x > 0.24$, where segregation occurs into Fe-rich regions exhibiting a net moment and Cr-rich regions with no net moment. Favorable and frustrated interatomic exchange interactions are revealed by their roles in defining these three structural regions through free-energy considerations. Generally the FM and SDWAFM order of elemental Fe and Cr do not mix. Fe-Fe FM exchange dominates magnetic order at T_R and is the source of magnetization in the alloys.

In region I a ferrimagnetic exchange between Fe and Cr stabilizes a local Cr moment, unlike the SDW origin of AFM moments in pure Cr. At $x = 0.91$ this exchange is associated with chemical short-range ordering in which Cr is surrounded only by Fe in the first-neighbor shell. As x decreases Cr-Cr nearest neighbors frustrate this chemical/magnetic order and Cr clustering or segregation ensues, reducing the net Cr moment. Cr-rich regions are not magnetically ordered as discussed below. The Fe-Fe FM exchange is not significantly perturbed at dilute Cr concentration, and remains intact as Cr segregates in region I. The energy of Fe-Fe exchange evidently is the driving force for segregation. Similar segregation behavior is observed in Co-Cr alloys in the Co-rich region,²¹ underlying interest in this and related alloy films for magnetic recording media.

The σ' phase is not stabilized by the energy of magnetic exchange interactions at T_R . We suggest that entropy associated with melting of assumed low- T ferrimagnetic ordered spins and the generally large degeneracy of possible d -electron configurations stabilizes the σ' phase, and also the high- T bulk σ phase. The metastability of σ' is evident in that it is not an end-point phase for segregation in region I or III. If it were an end-point phase in region I, a more rapid drop in Fe m_S would be expected. If it were an end-point phase in region III, no Fe magnetization would be observed. Indeed the relatively large Fe m_S (with $m_R \cong 0$) at $x = 0.5$ indicates that this composition is just outside the σ' boundary. In region III segregation into Fe-rich regions is again

driven by the Fe-Fe exchange interaction. The absence of a Cr net moment is consistent with AFM Cr order. However, Cr-rich regions in films with $x \geq 0.24$ are expected to exhibit no magnetic order, since even bulk alloys have T_N below T_R except for $x < 0.02$. Size effects would also suppress T_N below T_R even in otherwise pure Cr.^{9,22} The small size and possible Fe content of Cr-rich segregated regions make SDWAFM order unlikely at T_R .

Segregation in regions I and III is driven primarily by exchange energy gained in the FM ordering of Fe. Magnetic ordering of Cr does not provide a driving force for segregation, although added Cr beyond $x \approx 0.9$ spoils FM order in Fe thereby promoting segregation. Segregation proceeds readily at nanometer scales in sputter-deposited thin films because the kinetic energy of condensing species enhances add-atom mobility at the growing surface. These eased kinetic constraints together with possible stresses in growing films may explain the stability of σ' at T_R compared to the high- T stability of the bulk σ phase. Segregation is consistent with chemically distinct layers in Fe/Cr giant magnetoresistance multilayers,¹⁻³ while ferrimagnetic ordering of dilute Cr in Fe is consistent with surface alloying of Cr on Fe (001).^{7,8}

The reduced squareness of Fe could result from anisotropy, either from randomly oriented crystallites containing Fe-rich FM segregated regions, or from a tendency toward out-of-plane anisotropy. However $1 - S > 0$ whenever segregation occurs, suggesting that segregation is linked to its origin. Noncollinear Fe moments would result from frustrated Fe-Fe interatomic exchange interactions at segregation interfaces in which some interfacial Fe moments are weakly

coupled to the core of FM regions with noncollinear remnant orientation. This is consistent with bistable coupling of Fe to Cr(001) induced by structural disorder,¹¹ with segregated alloys exhibiting a wider range of disorder and hence switching fields. Alternatively, noncollinear coupling between segregated FM regions, similar to Fe/Cr multilayers,^{9,10} could yield reduced squareness. The squareness of Cr loops in region I is best reconciled by concluding that the Cr magnetization results from configurations of Cr dissolved into Fe-rich FM regions, and the reduced squareness of Fe results from weakly coupled moments at segregation interfaces at which intermixed Cr is predominantly paramagnetic. For $x \leq 0.50$ the second mechanism may be more appropriate.

The soft x-ray MO and scattering techniques utilized here have provided significant new information regarding element- and field-resolved magnetic and chemical order to reveal the roles of energetic and kinetic factors in determining metastable microstructures. Few if any other techniques are sensitive to these aspects of magnetism in films only 10 s of nanometers thick. Strong core resonances make these x-ray techniques generally applicable to a broad range of samples that need not be highly ordered.

We thank J. Bowers for assistance in sample preparation. Soft x-ray measurements were made at bending magnet beamlines 9.3.2 and 6.3.2 at the Advanced Light Source at LBNL. This work was supported by the Director, Office of Science, Office of Basic Energy Sciences, Materials Sciences Division of the U.S. Department of Energy under Contract No. DE-AC03-76SF00098.

*Visiting from Institut fuer Angewandte Physik, Universitaet Duesseldorf, 40225 Duesseldorf, Germany.

¹M. N. Baibich, J. M. Broto, A. Fert, F. Nguyen Van Dau, F. Petroff, P. Etienne, G. Creuzet, A. Friederich, and J. Chazelas, *Phys. Rev. Lett.* **61**, 2472 (1988).

²S. S. P. Parkin, N. More, and K. P. Roche, *Phys. Rev. Lett.* **64**, 2304 (1990).

³E. E. Fullerton, M. J. Conover, J. E. Mattson, C. H. Sowers, and S. D. Bader, *Appl. Phys. Lett.* **63**, 1699 (1993).

⁴J. Unguris, R. J. Celotta, and D. T. Pierce, *Phys. Rev. Lett.* **67**, 140 (1991).

⁵F. U. Hillebrecht, Ch. Roth, R. Jungblut, E. Kisker, and A. Bringer, *Europhys. Lett.* **19**, 711 (1992).

⁶Y. U. Idzerda, L. H. Tjeng, H.-J. Lin, C. J. Gutierrez, G. Meigs, and C. T. Chen, *Phys. Rev. B* **48**, 4144 (1993).

⁷A. Davies, J. A. Strocio, D. T. Pierce, and R. J. Celotta, *Phys. Rev. Lett.* **76**, 4175 (1996).

⁸B. Heinrich, J. G. Cochran, D. Venus, K. Totland, C. Schneider, and K. Myrtle, *J. Magn. Magn. Mater.* **156**, 215 (1996).

⁹E. E. Fullerton, K. T. Riggs, C. H. Sowers, S. D. Bader, and A. Berger, *Phys. Rev. Lett.* **75**, 330 (1995); E. E. Fullerton, S. D. Bader, and J. L. Robertson, *ibid.* **77**, 1382 (1996).

¹⁰A. Azevedo, C. Chesman, S. M. Rezende, F. M. de Aguiar, X. Bian, and S. S. P. Parkin, *Phys. Rev. Lett.* **76**, 4837 (1996).

¹¹E. J. Escoria-Aparicio, H. J. Choi, W. L. Ling, R. K. Kawakami, and Z. Q. Qiu, *Phys. Rev. Lett.* **81**, 2144 (1998).

¹²Reviews of structural and magnetic properties of Fe-Cr alloys can be found in *Numerical Data and Functional Relationships in Science and Technology*, Landolt-Börnstein, New Series III,

Vol. 19A (Springer-Verlag, Berlin, 1986), and Vol. 32A (1997).

¹³I. Mirebeau, M. Hennion, and G. Parette, *Phys. Rev. Lett.* **53**, 687 (1984).

¹⁴K. Saiki, K. Saito, K. Onishi, T. Numata, S. Inokuchi, and Y. Sakurai, *IEEE Trans. Magn.* **21**, 1471 (1985).

¹⁵K. Takanashi, T. Sugawara, K. Hono, and H. Fujimori, *J. Appl. Phys.* **76**, 6790 (1994).

¹⁶J. A. Aboaf and E. Klokholm, *IEEE Trans. Magn.* **17**, 3160 (1981).

¹⁷J. B. Kortright, M. Rice, and R. Carr, *Phys. Rev. B* **51**, 10 240 (1995).

¹⁸The polarization averaged absorption length at the Fe L_3 line is only 20 nm, so that unwanted spectral components in the incident beam can preclude precise absorption and MCD determinations in transmission. Such thickness effects were observed with differing severity from the same sample measured on different beamlines and with different gratings. Spectra in Fig. 1 are those least impacted by these effects.

¹⁹J. B. Kortright, M. Rice, S.-K. Kim, C. C. Walton, and T. Warwick, *J. Magn. Magn. Mater.* **191**, 79 (1999).

²⁰See, for example, D. De Fontaine, in *Solid State Physics: Advances in Research and Applications*, edited by H. Ehrenreich, F. Seitz, and D. Turnbull (Academic, New York, 1979), Vol. 34, p. 73.

²¹D. J. Rogers, Y. Maeda, K. Takei, J. N. Chapman, F. P. C. Bernardis, and C. P. G. Schrauwen, *J. Magn. Magn. Mater.* **130**, 433 (1994).

²²M. R. Fitzsimmons, J. A. Eastman, R. B. Von Dreele, and L. G. Thompson, *Phys. Rev. B* **50**, 5600 (1994).